

Design of Fresnel lenses and binary-staircase kinoforms of low value of the aperture number

Javier Alda ^{a,*}, José M. Rico-García ^a, José M. López-Alonso ^a,
Brian Lail ^b, Glenn Boreman ^c

^a Optics Department, University Complutense of Madrid, School of Optics, Av. Arcos de Jalón s/n, 28037 Madrid, Spain

^b Department of Electrical and Computer Engineering, University of Central Florida, P.O. Box 162450, Orlando, FL 32816-2450, USA

^c College of Optics and Photonics, CREOL, University of Central Florida, P.O. Box 162700, Orlando, FL 32816-2700, USA

Received 23 March 2005; received in revised form 25 October 2005; accepted 27 October 2005

Abstract

The design of plane Fresnel zone plates, and binary-staircase kinoforms, has been analyzed in this paper for a non-imaging application aimed to increase the performance of point-like detectors. They maximize the irradiance at the focal point of the diffractive element maintaining some constraints in the lateral size of the element. The design of the binary-staircase kinoform has been described as an iterative process. Some interesting results have been obtained for the values of the relative aperture number, or $F/\#$. The practical case treated here produces elements with very low $F/\#$. The results show that the gain of the irradiance at the focal point increases with the focal distance of the binary-staircase kinoform, and decreases with the focal length for a plane Fresnel zone plate having a limited lateral size. The calculation of the width of the irradiance distribution makes it possible to select those solutions that best concentrate the irradiance on the focal plane.

© 2005 Elsevier B.V. All rights reserved.

1. Introduction

Fresnel lenses are typically used to focus, or reshape, the irradiance distribution on detectors, and focal planes, in several electromagnetic bandwidths [1–4]. Some other solutions involving refractive lenslet arrays can be used [2], but they require a separate manipulation to align and integrate them with the detectors. The situation treated in this paper is a simple non-imaging application where the use of diffractive elements may change drastically the capabilities of a given technology. This is the case for infrared antennas. An interesting feature of infrared antennas is their point-like characteristic [5,6]. So far, we may say that optical and infrared antennas are the light detection technology having the smallest responsivity area ($\sim \lambda_0^2$, being λ_0 the detection wavelength). Typically, when infrared antennas are used for infrared imaging applications they are pat-

terned as a two-dimensional array at the location of the focal plane of the imaging optical system. The collected energy focused on a given individual detector can be increased by using diffractive non-imaging optics. In a previous contribution [7], it was proved that infrared antennas improve their responsivity, and the value of their normalized responsivity D^* , when customized Fresnel zone plates (FZP) are coupled to them. The responsivity is defined as the signal, in current or voltage, for a given incident optical power [8]. On the other hand, the normalized responsivity is defined as $D^* = \frac{\sqrt{A}\sqrt{\Delta f}}{\text{NEP}}$, where A is the detection area, Δf is the frequency bandwidth of the electronic subsystem used in the detection, and NEP is the noise equivalent power, defined as the power of the signal that produce a signal-to-noise ratio equal to 1 [8]. In the case of FZP coupled to infrared antennas, both the detector and Fresnel lenses were made using electron beam lithography, and integrated on the same double side, double polished, Si wafer. As far as that paper was aimed to prove the integrability of diffractive optics with the detection device on the

* Corresponding author. Tel.: +34913946874; fax: +34913946885.
E-mail address: j.alda@opt.ucm.es (J. Alda).

same element, there were no conditions about the lateral size of the FZPs. However, several applications involving the use of FZP are constrained by dimensional limitations for the transverse size of the FZP located in front of the detector. This is the case of focal plane arrays (FPA) composed of infrared antennas. The pitch of the FPA determines a maximum pixel's size. Moreover, this spatial period fixes, along with the characteristics of the optical system used to collect the energy and form the image, the resolution and sampling limitations of the system. On the other hand, the focusing gain of the Fresnel lens increases with the number of Fresnel zones. However, for a fixed transverse dimension of a plane FZP lens, the number of zones decreases when the focal length of the lens increases. This means that those Fresnel lenses having a large value of the $F/\#$ are not very well suited for its use for high-gain coupling applications. In this paper we define the aperture number, or f -number, for an object at the infinity as $F/\# = f/D_{EP}$, where f is the focal length of the system, and D_{EP} is the diameter of the entrance pupil. In our case D_{EP} can be considered as the lateral size of the diffractive element. To optimize the design of low- $F/\#$ diffractive elements, even within the scalar approximation, a more detailed solution is required. Our attention has been focused on a three-dimensional diffractive element: a binary-staircase kinoform [4,9]. The result is a diffractive solid immersion lens [10]. A previous analysis of this elements was done by us using a finite-differences in the time-domain algorithm (FDTD) [11]. One of the main conclusion of that paper is that the results obtained for the irradiance distribution from the FDTD were very close to the values obtained from the application of the Huygens–Fresnel principle [12], even when the spatial dimensions of the structure are only a little larger than the wavelength, and the application of the scalar diffraction approach could be compromised [13–16]. The comparison between the results of the scalar diffraction theory and the FDTD [11] shows the same trend observed by Bendickson et al. [16] for the irradiance of the focal plane of low f -number elements. For the case of plane Fresnel zone plate lenses of large $F/\#$ the fabrication was made by writing the zones on the surface of a double polished silicon wafer. The center of the FZPL was aligned with respect to the location of the infrared antenna. In this case, we propose the fabrication of the binary-staircase kinoform by using, for example, micro-machining techniques [17] or diamond turning machines [18] prior to the fabrication of the antenna, in order to preserve the detector as much as possible from the adverse effects of the fabrication method.

In this paper, we analyze the design of two types of diffractive elements: a Fresnel zone plate, and a binary-staircase kinoform. The geometric parameters defining the Fresnel zones have been obtained from optical path calculations [10]. The analysis has been done by computing the propagation of the wavelets produced at the location of the Fresnel zones within the scalar approximation. The incoming radiation is modelled as a plane wave propagat-

ing along the optical axis of the diffractive element. For the planar FZP the characteristics of the design are quite simple and some discussion about the feasibility of the design are analyzed in Section 2. In Section 3, we have analyzed a special type of kinoform constructed with concentric annuli located in a staircase arrangement, this diffractive element is named along the paper as a binary-staircase kinoform. The maximum departure of the phase shift is limited to π . The conditions established for the optical path determine the actual dimensions of the binary-staircase kinoform structure. We obtain here several constraints about the geometry of the successive Fresnel zones. The proposed design maximizes the number of zones of the kinoform. An iterative procedure is propose to obtain the optimized design. A practical case applicable to the binary-staircase kinoform made of Si and working at $\lambda_0 = 10.6 \mu\text{m}$ is presented. The gain in irradiance due to the diffractive element is calculated as a function of the focal length. A detailed analysis of the optimum solution is made within the scalar diffraction approach. This analysis provides a design having the minimum focal length, and the minimum $F/\#$ for a given number of zones in the binary-staircase kinoform. This design also optimizes the concentration of the irradiance around the focal point of the kinoform. Finally, Section 4 summarizes the main conclusions of the paper.

2. Fresnel lenses arranged as planar Fresnel zone plates

When considering the design of Fresnel lenses for micro-optics applications we are typically restricted to the selection of a very few parameters: the transverse size of the lens, $2R$ (being R the maximum radius of the Fresnel lens), the focal length, f , and the refractive index of the material used to fabricate the lens itself, n . Due to their diffraction mechanism, there is another parameter that plays a decisive role in the design of the lens: the wavelength in vacuum of the incoming radiation, λ_0 .

The Fresnel lens is defined by the Fresnel zones. These zones are defined by computing the optical path from the object to the image points and allowing a maximum departure of $\lambda_0/(2n)$. For a FZP working with an object placed at infinity, the Fresnel zones are placed on a plane located at a distance f from the focal point (see top of Fig. 1). The radius of the zones are given by the following expression:

$$r_m = \sqrt{\frac{m\lambda_0 f'}{n} + \frac{m^2 \lambda_0^2}{4n^2}}. \quad (1)$$

If the focal length is much larger than the transverse size of the lens (large $F/\#$) then the last term within the square root can be neglected with respect to the first one. Most applications of micro-optics Fresnel lenses are for an object at infinity. Therefore, the image is located at the focal point of the lens. This type of lens serves for the task of collecting the incoming energy onto a given area where the detector is placed. Due to the limitations in the transverse size

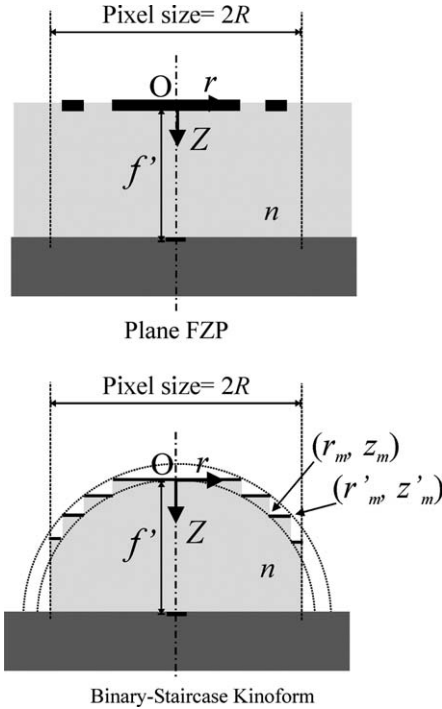


Fig. 1. Graphical layout of a planar FZP and a binary-staircase kinoform. The optical axis of the diffractive elements is the rotational symmetry axis, Z .

$(r_m \leq R, \forall m)$ the maximum number of Fresnel zones, M , is also limited and is given by

$$M = \frac{2n}{\lambda_0} \left[\sqrt{f'^2 + R^2} - f' \right] = \frac{4nR}{\lambda_0} \left[\sqrt{F\#^2 + \frac{1}{4}} - F\# \right], \quad (2)$$

where we have used $F\#$ to denote the relative aperture number, or f -number, $F/\#$ (this has been done to avoid misinterpretations in the reading of the equations). The absolute maximum for the number of zones of a plane Fresnel lens is obtained when considering a lens having a focal length $f' \rightarrow 0$ (this is equivalent to consider $F/\# \rightarrow 0$)

$$M_{\max} = \frac{2Rn}{\lambda_0}. \quad (3)$$

From previous results, it is known that the efficiency gain of the Fresnel lens will be larger when the $F/\#$ decreases and the FZP lens involves more Fresnel zones [7]. However, the contribution of each zone decreases as the zone is located farther from the center of the Fresnel lens because of the obliquity factor in the calculation of the contribution of the individual wavelets to the field on the focusing region. On the other hand, a plane FZP with adjacent zones showing a corresponding phase difference of π is usually fabricated having a squared profile with non-negligible thickness (actually, the thickness of the profile of a pure-phase FZP is $\lambda_0/(2n)$). Even for a plane FZP with obscured zones, some material has to be deposited to block the incoming light. For very low $F/\#$ lenses, the thickness of the profile of the plane FZP may be comparable to the focal length or the lateral extension of the Fresnel zone.

In this case, the obscuration between adjacent Fresnel zones may preclude the contribution of those zones located far from the center of the optical axis. Then, the results obtained from optical path calculations within the scalar treatment is just an approximation. Therefore, in practice, both the obliquity factor and the obscuration effect are limiting factors for the maximum size of the Fresnel lens designed as a plane plate. The gain factor of the diffractive element, GF, is defined as the ratio between the irradiance, I , with and without diffractive element, at a given point on the focal plane (described by r_d). It can be written as

$$GF(r_d) = \frac{I_{\text{with diffractive element}}(r_d)}{I_{\text{without diffractive element}}(r_d)}. \quad (4)$$

In Fig. 2, we have computed the gain factor for a collection of planar FZP with varying focal length. The incoming radiation is a uniform plane wavefront incident normally onto the FZP, and GF is calculated at the focal point, $r_d = 0$. The wavelength in vacuum is $\lambda = 10.6 \mu\text{m}$, and the material supporting the FZP is Si. This material is transparent for the analyzed wavelength and has an index of refraction $n = 3.42$. The irradiance is calculated by adding all the electric field amplitude contributions of the forward propagating wavelets. The complex electric fields are added, and then the irradiance is obtained after squaring the modulus of the resulting electric field. The irradiance without diffractive element is calculated by propagating a non-apertured infinite plane wave. The result, $I_{\text{without diffractive element}}$, is taken as the reference for all the cases having a diffractive element. The irradiance obtained for the diffractive element is calculated taking into account only the plane wave incident onto the diffractive element. All the planar FZPs represented in

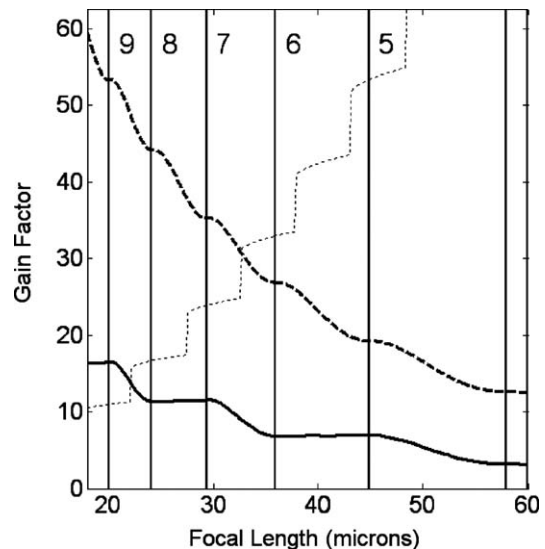


Fig. 2. The gain factor decreases when f' increases. The solid line is for a plane FZP having alternated obscured Fresnel zones (the central zone is open). The dashed line is for a pure phase planar FZP. The number inside the graphic area represent the number of Fresnel zones. The dotted line is the GF calculated for the binary-staircase kinoforms designed in this paper. Here, it is shown for comparison.

Fig. 2 have the same limitation in their transverse size, $2R = 55 \mu\text{m}$. The solid line is for plane FZPs having alternated obscured Fresnel zones (the central one is open), and the dashed line is for pure-phase planar FZPs. In this last case we have neglected the obscuration effect due to the finite thickness of the phase profile. From this plot, we conclude that GF decreases with f' because the number of Fresnel zones, for a fixed lateral dimension, is also decreasing when f' increases. The vertical solid lines represent the change in the number of Fresnel zones. In the analyzed case, the FZPs have a number of Fresnel zones ranging from 4 to 10. The dotted line represents, as a function of the focal length, the GF for the binary-staircase kinoform designed in the following section.

3. Three-dimensional Fresnel lenses. Binary-staircase kinoforms

Another kind of diffractive element used in micro-optics applications are those where the Fresnel zones are located in a three-dimensional arrangement [4]. The elements obtained using this three-dimensional arrangement can be classified as a binary-staircase kinoform [9], or a diffractive immersion lens [10]. The kinoforms treated in this contribution consist of a sequence of Fresnel zones configured as flat parallel steps each having an annular shape (even the first one could be considered as a circular annulus having an internal radius equal to zero). The phase difference between the optical path from the two limits of every step is π . In the bottom of Fig. 1, we show the spatial arrangement of the kinoform and how the cylindrical coordinate system is configured. The global shape of the element analyzed in this paper is convex. However, it could be also possible to define a concave binary-staircase kinoform having the same focalization behaviour. The effect of the obscuration between adjacent zones could be more relevant for the concave case than for the convex one. The steps of our convex binary-staircase kinoform are plane interfaces separating two media having different index of refraction, n_{ext} , and n (where n_{ext} denotes the index of refraction of the medium where the incident wavefront is coming from). The dimensions of these steps are one of the results of the design process. For each Fresnel zone, the internal points of the annulus corresponding to the zone labelled with index, m , are given by coordinates (r_m, z_m) , and the external points are given by (r'_m, z'_m) . The design process has to produce the values of these geometric variables optimized for a maximum radiometric efficiency of the kinoform computed from optical path calculations within the scalar approximation. Although the design approach is purely geometric [10], a more accurate description of binary-staircase kinoforms using finite-differences in the time-domain (FDTD) methods provide more accurate results. The FDTD results locate the focus of the kinoform in the same location obtained from optical path evaluation, approximately [11]. This result is in good accordance with the conclusions obtained by Bendickson et al. [16] for the case of the irra-

diance distribution at the focal plane of a diffractive lens, where they found less discrepancies between the exact and the scalar diffraction approach.

Let us assume that light is incident as a monochromatic plane wave having a wave vector, \vec{k} , parallel to the optical axis of the diffractive element. This choice is made because we pay special attention to the practical case of collecting the irradiance coming from the infinity, and focusing it onto the focal point of the kinoform. This point will be the location of the point-like detector. The extension of the Fresnel zone is given by the same condition about the optical path difference used for the typical design of plane Fresnel lenses. In this case, the optical path difference has to take into account the optical path travelled from a given reference plane. Without loss of generality this reference plane is located at a distance f' from the focus. The limit of the zone m is reached when the geometrical path obeys the following condition:

$$\sqrt{r_m'^2 + (f' - z_m')^2} = \sqrt{r_m^2 + (f' - z_m)^2} + \frac{\lambda_0}{2n}, \quad (5)$$

where the square root on the right-hand side of the equation represents the geometrical path from the inner limit of the zone to the focal point, and the square root of the left-hand side of this equation represents the geometrical path for the outer limit of the same Fresnel zone. The geometric path difference is established in this equation as $\lambda_0/2n$. The previous equation involving geometrical paths holds true because the wavelength has been shrunk by the factor n . However, any other condition to produce a finer quantization of the optical path can be set by changing the $1/2n$ factor to another suitable value. From this equation, we may obtain the value of the radius of the first zone r'_1 . This equation produces the same result than (1) only for the first zone ($m = 1$, assuming that $r_1 = 0$, and $z_1 = 0$). Due to the staircase arrangement of the zones we may assure that

$$z'_m = z_m. \quad (6)$$

The next zone, $m + 1$, begins where the previous finishes, but at a different height. This means that

$$r_{m+1} = r'_m. \quad (7)$$

Besides, the optical path from the beginning of the following zone to the focal point has to be equal to the optical path from the beginning of the previous zone to the focal point. Then, by applying this recurrence, this optical path is equal to nr' , that is the optical path from the center of the first zone to the focal point. This condition can be generalized to obtain the distance from the reference plane of the successive Fresnel zones, z_m (where $m = 2, \dots, M$), as

$$nr' = n\sqrt{r_m^2 + (f' - z_m)^2} + n_{\text{ext}}z_m. \quad (8)$$

Geometrical interpretations can be obtained from the previous conditions. Eq. (8) establishes the internal limits of the Fresnel zones. Eq. (5) defines the external limits of the Fresnel zones. After some algebra, the curve for the internal points of the Fresnel zones is written as

$$z = \frac{nf'}{n + n_{\text{ext}}} \left[1 - \sqrt{1 - \left(\frac{n + n_{\text{ext}}}{n - n_{\text{ext}}} \right) \frac{r^2}{f'^2}} \right], \quad (9)$$

where we are assuming that $n_{\text{ext}} < n$. The curve defining the outer limit of the Fresnel zone is obtained from Eq. (5) and condition (6), and is given by

$$z' = f' - \frac{n}{\lambda_0} \sqrt{\left[r'^2 - r^2 - \left(\frac{\lambda_0}{2n} \right)^2 \right]^2 - \left(\frac{\lambda_0 r}{n} \right)^2}. \quad (10)$$

By using Eqs. (9) and (10), we define a region where the annular steps fall.

As we have seen, Eq. (8), is used to define the inner radius of each Fresnel zone. This condition defines a stigmatism correspondence between a centered point at the infinite and another point immersed in the second medium and located at f' . A simple algebraic transformation of this relation gives the equation of a conicoid surface of the type $r^2 = 2\rho_0 z - pz^2$. This surface has a radius of curvature at the vertex, $\rho_0 = f'(n - n_{\text{ext}})/n$, that is equal to the radius of curvature of a spherical dioptric surface having its focal point at f' . The asphericity parameter, $p = 1 - n_{\text{ext}}^2/n^2$, corresponds with that of a prolate ellipsoid ($0 < p < 1$). This means that the curve described by Eq. (9) is wider than its tangent sphere (the tangent sphere can be obtained by substituting $p = 1$ in the conicoid equation). Eq. (9) can be used to obtain some other important relations. This equation contains a square root which has to produce a real valued result. Then, the term inside the square root has to be greater than zero. Therefore

$$r \leq r_{\text{max}} = f' \frac{n - n_{\text{ext}}}{n + n_{\text{ext}}}. \quad (11)$$

This condition implies a relation between the transverse size of the Fresnel zone and the focal length when the size is limited by the previous condition. This relation can be written in terms of the numerical aperture as follows:

$$F\# \geq \frac{1}{2} \sqrt{\frac{n + n_{\text{ext}}}{n - n_{\text{ext}}}}. \quad (12)$$

The term inside the square root is related with the reflectance of the lens medium and the external medium interface, $\mathcal{R} = \left(\frac{n - n_{\text{ext}}}{n + n_{\text{ext}}} \right)^2$. By using this relation, Eq. (12) becomes

$$F\# \geq \frac{1}{2} \mathcal{R}^{-1/4}. \quad (13)$$

The evolution of this minimum value for $F\#$ as a function of the index of refraction of the material used to fabricate the lens is plotted in Fig. 3. It should be noted that for the case of infrared materials, the index of refraction is typically larger than in the visible. Then, the reflectance is larger than in the visible and the inequality (13) has a lower bound. This fact makes possible to produce lenses with lower $F\#$ in the infrared than in the visible. This means that, as the index of refraction of the material of the lens increases, the focusing capabilities improve and the maximum irradiance is larger. However, this trend is com-

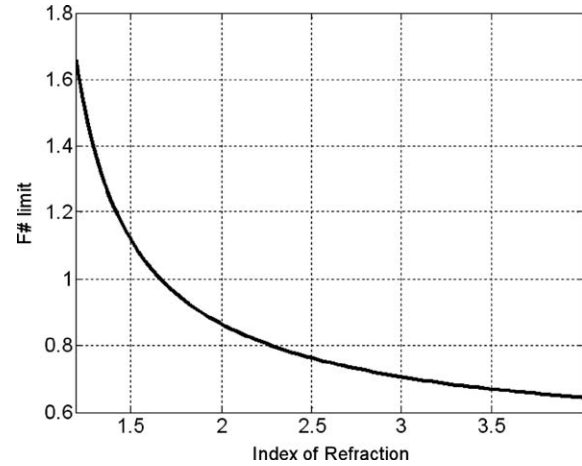


Fig. 3. Dependence of the minimum $F\#$ vs. the index of refraction of the material of the lens (assuming air as the external medium).

pensated by the increase in the reflection coefficient. On the other hand, the absolute minimum for $F\#$ has a more complicated dependence on the value of the focal length of the lens, as we will see in the following subsection.

3.1. Practical design of kinoforms with minimum $F\#$

In the previous paragraphs, we have presented a collection of equations and conditions determining the design of a binary-staircase kinoform. Now, we describe how this design may be realized in practice. We propose an iterative method that builds the kinoform one zone after the other beginning with the central one. This procedure needs the knowledge of the internal coordinates of the first zone. We set these coordinates as $r_1 = 0$ and $z_1 = 0$. The method itself will be applied starting at the first zone in a recurrent manner, until some design condition is reached and the iterative procedure stops. In the method presented here, the condition to stop the design maximizes the number of zones. This is because the irradiance at the focal point increases with the number of zones. At the same time, when the number of zones increases, the transverse dimension of the kinoform also increases and the $F\#$ decreases, reaching a minimum value.

The input of each iteration are the coordinates of the internal limit of the m zone, (r_m, z_m) . The method uses the fact that the Fresnel zones are located at parallel planes between the lines defined by Eqs. (9) and (10). This means that condition (6) has to be satisfied for each zone, and z'_m is easily obtained. Besides, the outer radius limiting a given Fresnel zone is obtained from condition (5) as

$$r'_m = \sqrt{r_m^2 + \frac{\lambda_0^2}{4n^2} + \frac{\lambda_0}{n} \sqrt{r_m^2 + (f' - z'_m)^2}}. \quad (14)$$

At this point we have the coordinates of the inner and outer limits of the zone m , (r_m, z_m) and (r'_m, z'_m) , respectively. The next zone begins where the previous one finishes. This condition has been described by Eq. (7). The height of this

following zone is given by the condition (8), that corresponds with Eq. (9). This last equation can be re-written using now the appropriate subindices as

$$z_{m+1} = \frac{nf'}{n + n_{\text{ext}}} \left[1 - \sqrt{1 - \left(\frac{n + n_{\text{ext}}}{n - n_{\text{ext}}} \right) \frac{r_{m+1}^2}{f'^2}} \right]. \quad (15)$$

The previous equations define the iterative procedure as the successive application of equations (6)–(14) and (7)–(15). The process stops when applying Eq. (15) the solution is complex for a given $m + 1 = M + 1$. This happens when

$$r'_M = r_{M+1} > r_{\text{max}}, \quad (16)$$

where r_{max} is defined in (11). Therefore, the number of zones of the kinoform is M . In Fig. 4, we present the flow graph of the proposed iterative algorithm.

As a consequence of the previously proposed method of design, we may say that the last zone of the binary-staircase kinoform finishes at a point belonging to the curve (10). If we are interested in an element having the maximum number of zones possible, the iterative method is only stopped when no real value is obtained from Eq. (15). Depending on the value of the focal length, the actual radius of the outer limit of the kinoform, r'_M , is larger than, or equal to, r_{max} . Unfortunately, there is not an analytical form for

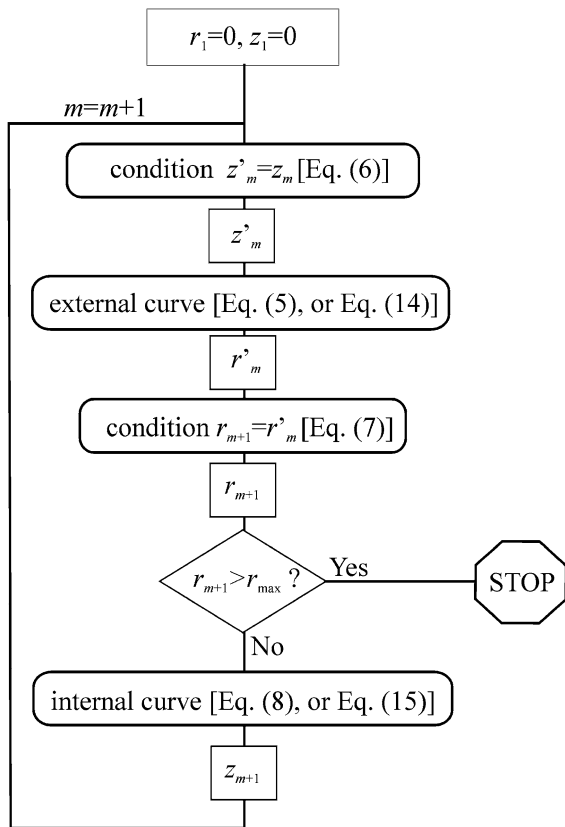


Fig. 4. Flow graph of the iterative method proposed to obtain the geometric parameters of the optimized binary-staircase kinoform. The method begins with the value of the inner points of the first zone, and stops when the external radius of the last zone is larger than the maximum allowed internal radius, r_{max} .

r'_M because it is obtained from an iterative process. In any case, the value of the $F/\#$ given by Eq. (13) can be considered as an upper limit for those kinoforms having the maximum number of zones possible.

In order to clarify these previous concepts, we have performed a numerical calculation of several designs of binary-staircase kinoforms. The physical parameters used in the design correspond with the practical situation of an element fabricated with Si, $n = 3.42$, operating at $\lambda = 10.6 \mu\text{m}$ (Si is transparent at this wavelength). We are assuming a plane wavefront incident normally onto the kinoform from the air. Fig. 5 shows that the $F/\#$ of the kinoform is between two limits. The upper limit corresponds with the condition of Eq. (13) that is not dependent on f' . The lower limit is depending on the focal length. The sharp changes in $F/\#$ are produced when the inner limit of the last zone is equal to r_{max} . The dashed line represents the condition limiting the diameter of the kinoform to $55 \mu\text{m}$ (as it was done for the plane FZP). The lenses located to the left of this dashed line represent binary-staircase kinoforms having a diameter smaller than $55 \mu\text{m}$.

The diffractive elements described in this paper are designed to increase the irradiance in its focal plane. Therefore, our interest is to know the behaviour at the focal plane of the binary-staircase kinoform compared with the situation without any element under the same incidence conditions. Fig. 6 represents the value of the gain factor of the binary-staircase kinoform as a function of its focal length. In Fig. 6, the selected point is the focal point, $r_d = 0$. We may see that the gain factor increases with the focal length. The vertical lines represent the transitions between elements having an additional Fresnel zone. It is interesting to note that the gain factor jumps to a higher value when the number of zones increases. This is because of the additional contribution of a new Fresnel zone. In Fig. 7, we compare in the same graph the physical layout and shape of two binary-staircase kinoforms, having

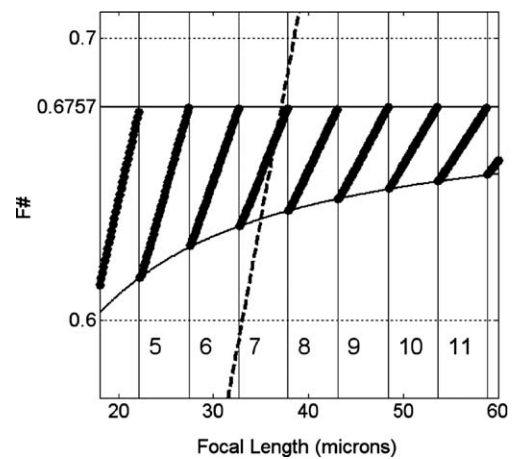


Fig. 5. Variation of the $F/\#$ as a function of the focal length. The numbers in the graphic area denote the number of Fresnel zones. Those binary-staircase kinoforms located to the left of the dashed line are those having a transverse size smaller than $55 \mu\text{m}$.

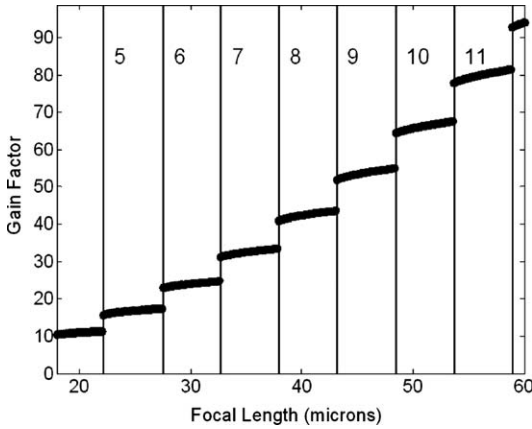


Fig. 6. The gain factor, GF, increases with the focal length. The vertical lines determine the regions with the same number of zones (denoted by numbers inside the graphic area). GF jumps abruptly when a new zone is added. Within those designs having the same number of zones, GF increases but at a smaller rate.

$M = 6$ (at the left), and $M = 7$ (at the right) Fresnel zones. This figure explains how the application of the iterative procedure may produce two kinoforms having very similar focal lengths, but having a different number of Fresnel zones, and therefore a different behaviour at the focal plane. In Fig. 8, we have represented the gain factor as a function of the position at the focal plane of the binary-staircase kinoform. This plot is proportional to the irradiance distribution at the focal plane and calculated under a scalar diffraction approximation. The curves represent the cases plotted in Fig. 7. The dotted line is for the case with $M = 7$, and the solid one is for $M = 6$. As we already proved in Fig. 6 the gain factor is larger for a larger number of zones, although the change in the focal length is very small. Another interesting remark is the change in the shape of the irradiance around the focal point. This fact can be seen in this figure and it is also parameterized with the calculation of the width defined with the second-order moments of $GF(r_d)$

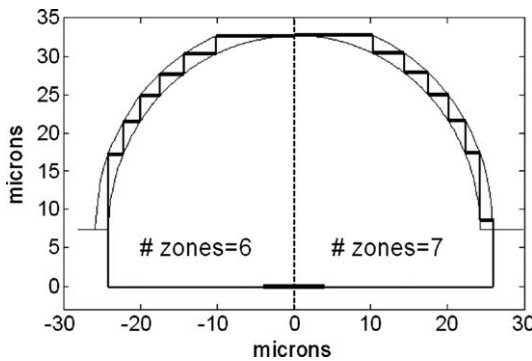


Fig. 7. This figure compares the actual profiles of two binary-staircase kinoforms. On the left of the optical axis, we have represented a binary-staircase kinoform having six Fresnel zones. On the right side, we have plotted a binary-staircase kinoform with seven Fresnel zones. These designs differs very little in focal length but the gain factor and their spatial distribution changes significantly.

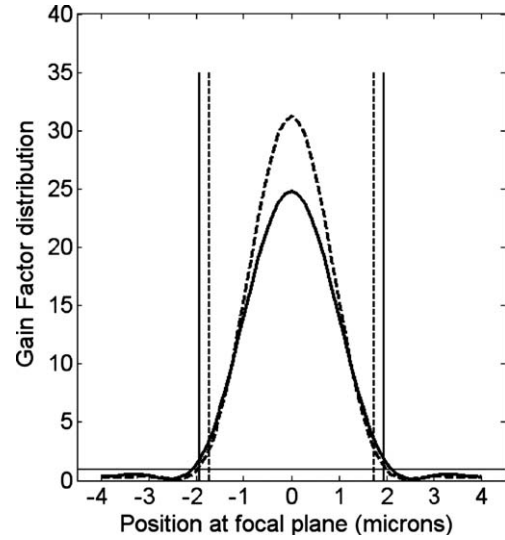


Fig. 8. The gain factor can be calculated at any location on the focal plane. It has a maximum at the center. The solid line represents the gain factor distribution for the design shown on the left side of Fig. 7. The dashed line is for the practical design represented on the right side of Fig. 7. Besides of an increase in the gain factor, we can see that the energy is more concentrated for the dashed line. The vertical lines plotted in this figure are located at the position of the calculated width for each distribution.

$$\omega = 2\sqrt{\frac{\int_{-\infty}^{\infty} GF(r_d)r_d^2 dr_d}{\int_{-\infty}^{\infty} GF(r_d) dr_d}} \tag{17}$$

This has been represented in Fig. 9 as a function of the number of zones. The meaning of this figure is that the irradiance is more concentrated (lower width) when $F/\#$ is smaller for a given value of the number of zones. The vertical solid lines connecting the large dots represent the evolution of the width as the focal length increases.

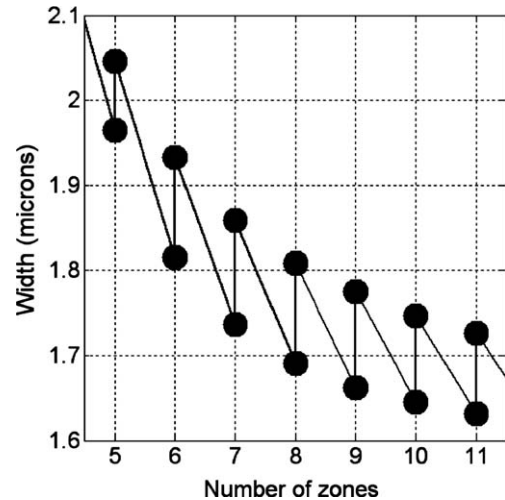


Fig. 9. Plot of the width calculated with the second-order moments as a function of the number of zones. The width is narrower for those binary-staircase kinoforms having a shorter focal length. The vertical solid lines between the circles represents the evolution of the width as the focal length increases for a constant number of Fresnel zones.

oblique solid lines only represent the connection between kinoforms having an additional Fresnel zone (no elements are defined having a non-integer number of Fresnel zones).

Summarizing the previous findings, we may conclude that the design of the binary-staircase kinoform can be optimized by selecting the focal length corresponding to the minimum value of the $F/\#$. This is because the most significant change in the gain factor is produced when an additional Fresnel zone appears. On the other hand, for those formats having the same number of zones, the gain factor increases, however, the width also increases and distributes the irradiance on a larger area.

4. Conclusions

In this contribution, we have presented a geometric analysis of the conditions defining the spatial dimensions of FZPs and binary-staircase kinoforms optimized to increase the irradiance on the focal point of the diffractive element and constrained by a bound in their lateral dimensions. These diffractive elements are capable to improve the electro-optical performance of optical and infrared antennas. The design of the diffractive element is based on geometric and optical path calculations. The treatment is made under the scalar diffraction approximation because a previous and more detailed analysis of the same type of elements using FDTD techniques produced results in good agreement with the expectations obtained from the scalar diffraction analysis. The illuminating source is a collimated uniform plane wave having a direction of propagation parallel to the optical axis of the diffractive elements. The analysis has begun with the case of a plane FZP. In this case, the transverse size limitation has been related to the total number of zones obtaining that, for a fixed lateral size, the number of zones increases as the focal length of the FZP decreases. We have made a more detailed analysis of a binary-staircase kinoform consisting of plane parallel circular annuli. The maximum departure in the phase between the limits of a given annulus is π . Within the design conditions, we have developed a sound iterative method to specify the dimensions of an optimized element. The method begins with the dimensioning of the first zone and obtains the spatial locations of the maximum number of Fresnel zones allowed.

The evaluation of the optical path for a uniform plane wave coming from infinity and focusing on the focal point of the binary-staircase kinoform has produced several interesting results. The first one is that the $F/\#$ for a binary-staircase kinoform with the maximum number of zones diminishes as the index of refraction of the material used to fabricate the binary-staircase kinoform increases. The actual $F/\#$ for the optimized case is ranging between a value that only depends on the index of refraction of the diffractive immersion lens and the index of refraction of the external medium, and another lower value that also depends on the focal length. The gain factor at the focal point, defined as the ratio between the irradiance with the

binary-staircase kinoform and without the kinoform at this focal point, increases with the focal length. The gain factor actually jumps to a higher level when an additional Fresnel zone is added to the design. On the other hand, the concentration of the irradiance is lowered when the focal length increases for a fixed value of the number of zones. This fact points out that the optimum binary-staircase kinoform is obtained for the minimum focal length at a fixed number of zones. This minimum focal length also corresponds with the minimum aperture number.

Finally, we may say that the gain factor has been obtained for a binary-staircase kinoform having plane interfaces between air and media. An important improvement of the design could be achieved if the kinoform is coated with an anti-reflection film. As far as the transmittance due to Fresnel reflection in the air/medium interface is equal to 0.7 for the material selected in this paper, the improvement in the gain factor could be a factor of $\times 1.42$ just by adding an appropriate anti-reflection thin film.

Acknowledgments

This work has been partially supported by the Project TIC2001-1259 of the Ministerio de Ciencia y Tecnología of Spain, and by a collaboration agreement between the University Complutense of Madrid and the University of Central Florida.

References

- [1] J. Ojeda-Castañeda, C. Gómez-Reino (Eds.), Selected Papers on Zone Plates, SPIE Press, Bellingham, WA, 1996.
- [2] H.P. Herzig (Ed.), Micro-optics. Elements, Systems and Applications, Taylor & Francis Ltd., London, 1997.
- [3] H.D. Hristov, Fresnel Zones in Wireless Links, Zone Plane Lenses and Antennas, Artech House, Norwood Mass, 2000.
- [4] I.V. Minin, O.V. Minin, Diffractive Optics of Millimetre Waves, Institute of Physics, Bristol, UK, 2004.
- [5] F.J. González, J. Alda, B. Illic, G. Boreman, IEEE J. Sel. Top. Quantum Electron. 11 (2005) 117.
- [6] J. Alda, J.M. Rico-García, J.M. Lpez-Alonso, G. Boreman, Nanotechnology 16 (2005) S230.
- [7] F.J. González, J. Alda, B. Illic, G. Boreman, Appl. Opt. 43 (2004) 6067.
- [8] G. Boreman, Basic Electro-Optics for Electrical Engineers, SPIE Optical Engineering Press, Bellingham, Washington, 1998.
- [9] J.M. Sasian, R.A. Chipman, Appl. Opt. 32 (1993) 60.
- [10] R. Brunner, M. Burkhardt, A. Pesh, O. Sandfuchs, M. Ferstl, S. Hohng, J.O. White, J. Opt. Soc. Am. A 21 (2004) 1186.
- [11] J.M. Rico-García, J.M. López-Alonso, B. Lail, G. Boreman, J. Alda, Proc. SPIE 5612 (2004) 216.
- [12] E. Hecht, Optics, Addison-Wesley, Reading, MA, 1998.
- [13] D.A. Pommet, M.G. Moharam, E.B. Grann, J. Opt. Soc. Am. A 11 (1994) 1827.
- [14] Z. Jaroszewicz, A. Kolodziejczyk, M. Sypek, C. Gómez-Reino, J. Mod. Opt. 43 (1996) 617.
- [15] I. Richter, Z. Ryzí, P. Fiala, J. Mod. Opt. 45 (1998) 1335.
- [16] J.M. Bendickson, E.N. Glytsis, T.K. Gaylord, J. Opt. Soc. Am. A. 15 (1998) 1822.
- [17] J.M. Bustillo, R.T. Howe, R.S. Muller, Proc. IEEE 86 (1998) 1552.
- [18] C.G. Blough, M. Rossi, S.K. Mack, R.L. Michaels, Appl. Opt. 36 (1997) 4648.